AD-A040 172 TETRA TECH INC PASADENA CALIF F/G 20/4
ANALYSIS OF DATA ON WATER WAVES. VOLUME III. SHALLOW WATER WAVE--ETC(U)
JUN 67 R W WHALIN DACA39-67-C-0022
UNCLASSIFIED TETRAT-TC-105-3 WES-CR-1-167-VOL-3 NL

| OF |
AD
A040172

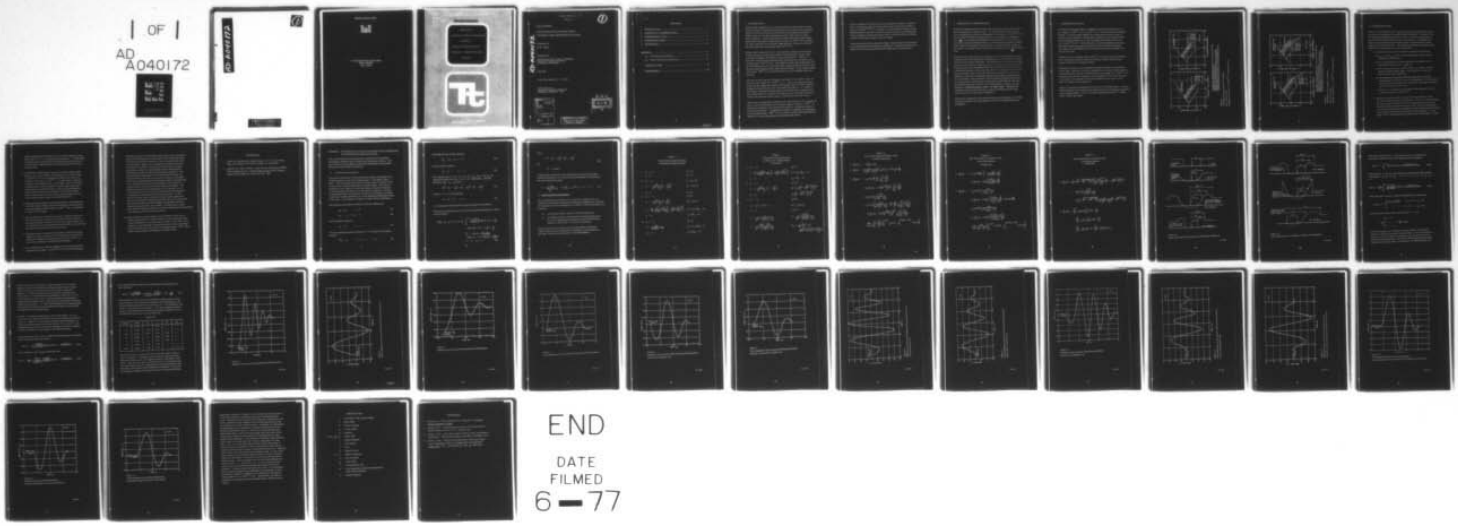

END

DATE
FILMED
6-77

FINAL REPORT

ANALYSIS OF DATA ON WATER WAVES

VOLUME III

SHALLOW WATER WAVE STUDY

Contract No. DACA 39-67-C-0022

June 1967

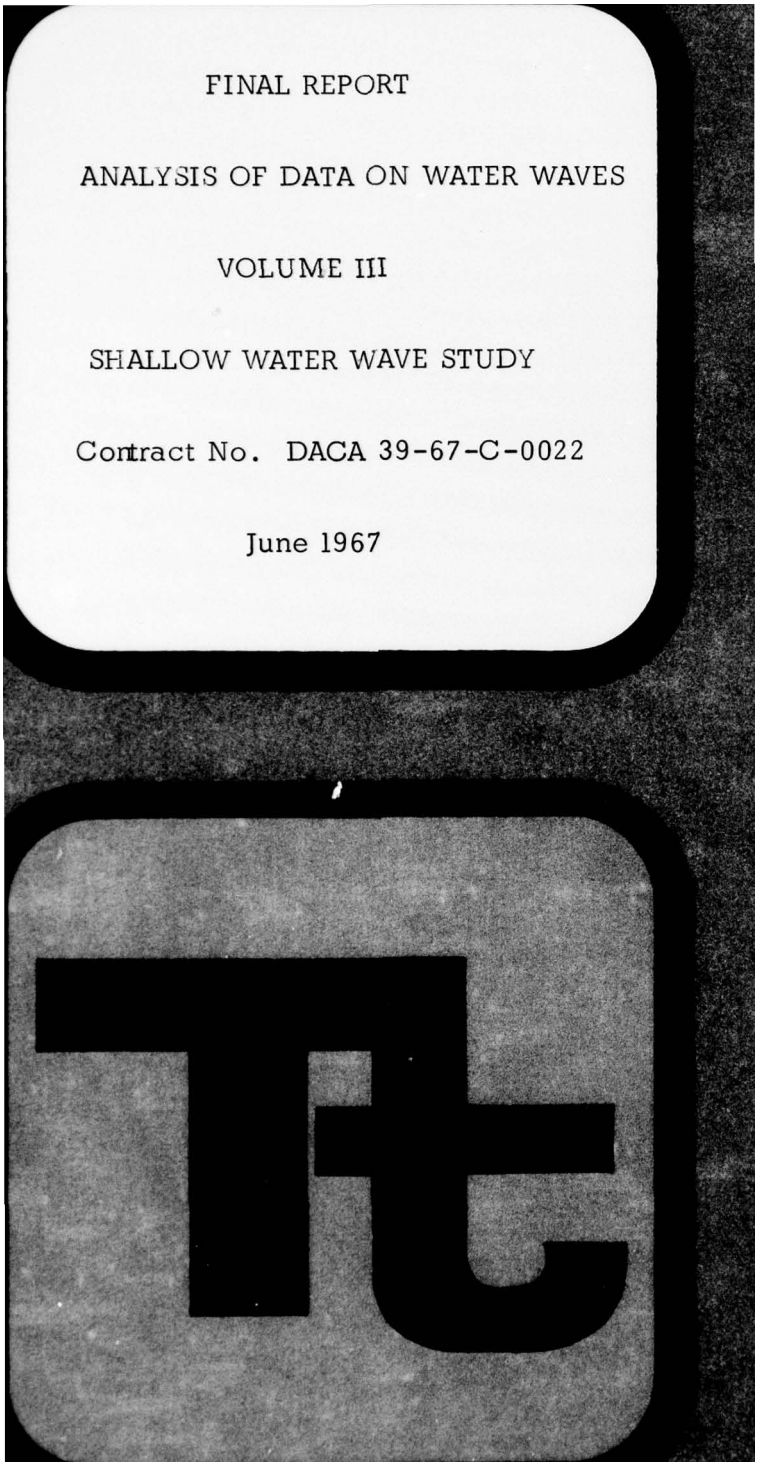

CONTRACT REPORT NO. 1-167

VOLUME III

(1)

FINAL REPORT

ANALYSIS OF DATA ON WATER WAVES

VOLUME III SHALLOW WATER WAVE STUDY

Prepared by:

R. W. Whalin

Prepared for:

United States Army Corps of Engineers
Waterways Experiment Station
Vicksburg, Mississippi

June 1967

Tetra Tech Report No. TC 105-3

Tetra Tech, Inc.
630 North Rosemead Boulevard
Pasadena, California 91107

AD-A040172

CONTENTS

1. INTRODUCTION

Shallow water explosions are commonly defined as detonations in water where the bottom influences the generation of the water waves produced. Until this test series performed by the Waterways Experiment Station (WES), there was no data indicating the water depth limit for a deep water explosion. Recent experimental studies indicate the water depth becomes an important consideration for values of $d/W^{1/3} \leq 4.0$ (d being the water depth and W the charge weight) and that it begins to influence the wave generation mechanism when $d/W^{1/3} < 6.0$.

Shallow water explosions were, until recently, thought of as producing a large amplitude solitary type initial crest followed by a long trough and higher frequency oscillations of decreasing period. However, it has been relatively well established that wave trains of this type are not produced until $d/W^{1/3} \lesssim 0.6$. This depth limit has been established from the 1955 WES test series, 1966 Mono Lake shallow water test series, and the present test series being conducted by the WES. In this report detonations where $d/W^{1/3} \leq 0.6$ will be referred to as very shallow water explosions.

The case of most interest and prime importance is for shallow water explosions in the range $0.6 < d/W^{1/3} \leq 6.0$. This is an extremely large range of water depths and includes the weapons in 1/2 - 50 MT range detonated at some location on the continental slope (800 ft. < d < 6000 ft.). The largest amplitude breaking waves will be produced by explosions at this location which is of utmost importance as far as damage potential to surface and subsurface ship traffic, littoral drift, and wave run-up.

Theoretical investigations of shallow water explosions are very limited and there is not sufficient data over the large range of values for $d/W^{1/3}$ to assess the reliability of any theoretical models or to produce empirical prediction techniques. A prediction technique is available for explosions in very shallow water ($d/W^{1/3} \lesssim 0.6$) and was constructed empirically by WES (Ref. 1) from data gathered by extensive test series.

Several mathematical models have been proposed by Whalin and Divoky (Ref. 2) which may apply to the transition zone from deep to shallow water ($0.6 \lesssim d/W^{1/3} \lesssim 6.0$). However, the assessment of these models depends upon the collection of extensive data necessary in evaluating the initial conditions (cavity parameters and/or velocity field) as a function of yield, submergence depth, and water depth.

The latter section of this report delineates experimental and theoretical areas needing further development leading to a reliable prediction technique of the water waves generated by explosions in shallow water.

2. THEORETICAL CONSIDERATIONS

Theoretical developments have been very limited for water waves generated by explosions in shallow water. An initial attempt which seems to show considerable promise for detonations in the range $0.6 \lesssim d/W^{1/3} \lesssim 6.0$ was developed by Whalin and Divoky (Ref. 2) and appears as Appendix I. This work is an attempt at extending the linear theory of water waves in an inviscid, incompressible medium, of constant depth to apply to shallow water explosions through the use of either a stationary initial surface deformation or an initial velocity field which is determined from experimental data.

Data from this test series can be used to assess the applicability of these mathematical models along with a modification of the presently available deep water prediction techniques. Of considerable interest are the mathematical models shown in Figures 12 and 13 of Appendix I which consist of stationary and a time dependent initial surface deformation in the form of a truncated parabolic cavity with a lip which is an extension of the cavity. This particular model is precisely the same evolved by Van Dorn and Whalin for deep water predictions when the water depth is greater than the cavity depth. Upon evaluation of this model with experimental data, it may be that one mathematical model will be applicable for both deep and shallow explosions with the cavity parameters η_o and R_o being a function of yield, submergence depth, and water depth. Obviously the evaluation of this model will entail a numerical integration for areas near the source as mentioned in Appendix I.

Should these extensions of the linear theory prove inadequate, non-linear theoretical models can be developed for both the wave generation and propagation.

3. EXPERIMENTAL DATA

All known experimental data on explosively generated water waves is for ranges of $d/W^{1/3} > 6.0$ or $d/W^{1/3} < 0.9$. This test series, although limited, is the only data available in the transition zone from deep to shallow water explosions. Preliminary indications of this data are that the maximum amplitude of the first envelope is reduced by 1/2 to 1/3 for $2 \lesssim d/W^{1/3} \lesssim 4.0$. This reduction is certainly significant and may drastically influence present conclusions on the severity of the wave environment on continental shelves produced by weapons detonated seaward of the shelf.

Explosions in very shallow water ($d/W^{1/3} < 0.6$) are of less importance due to the greatly reduced energy partitioned to water waves and consequent reductions in damage potential.

Unfortunately there is not enough data available to draw any conclusions at this time. However, of prime importance is a need for extensive tests (especially small yield less 1,000 lbs TNT) in the range $0.6 \leq d/W^{1/3} \leq 6.0$. One question of prime importance is the magnitude of the waves produced at the upper critical depth and even the existence of the upper critical depth for shallow water explosions.

Figures 1 and 2 show extrapolated curves from a 1955 WES report on Shallow Water Explosions for predicting the height of the first wave from explosions in very shallow water. Four curves are illustrated for $d/W^{1/3} = 0.088$, 0.175, 0.292, and 0.585.

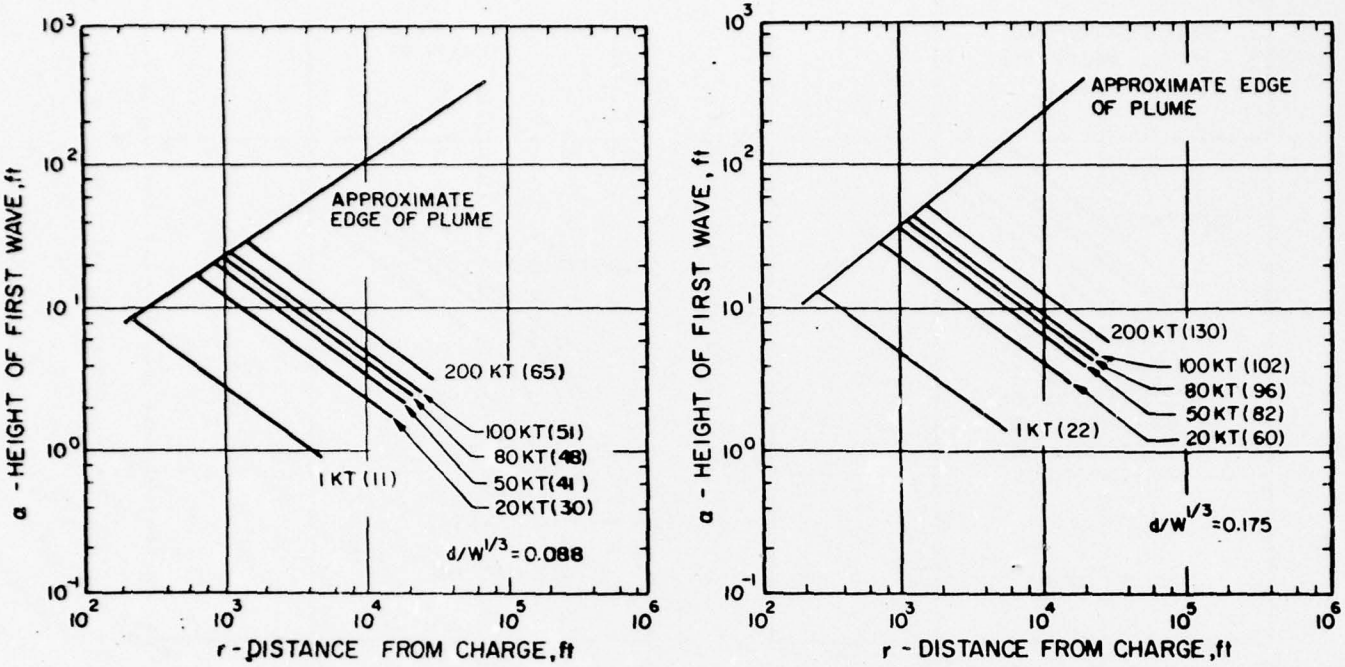

FIGURES IN PARENTHESES ARE ACTUAL WATER DEPTHS IN FEET FOR SPECIFIED YIELDS
ORIGINAL DATA UPON WHICH THESE CURVES ARE BASED EXHIBITED A SCATTER OF APPROXIMATELY ±30% STANDARD DEVIATION OF A SINGLE OBSERVATION

Figure 1

Variation of wave height with distance

for various yields

charge at surface (Z = 0) $d/W^{1/3}$ = 0.088 and 0.175

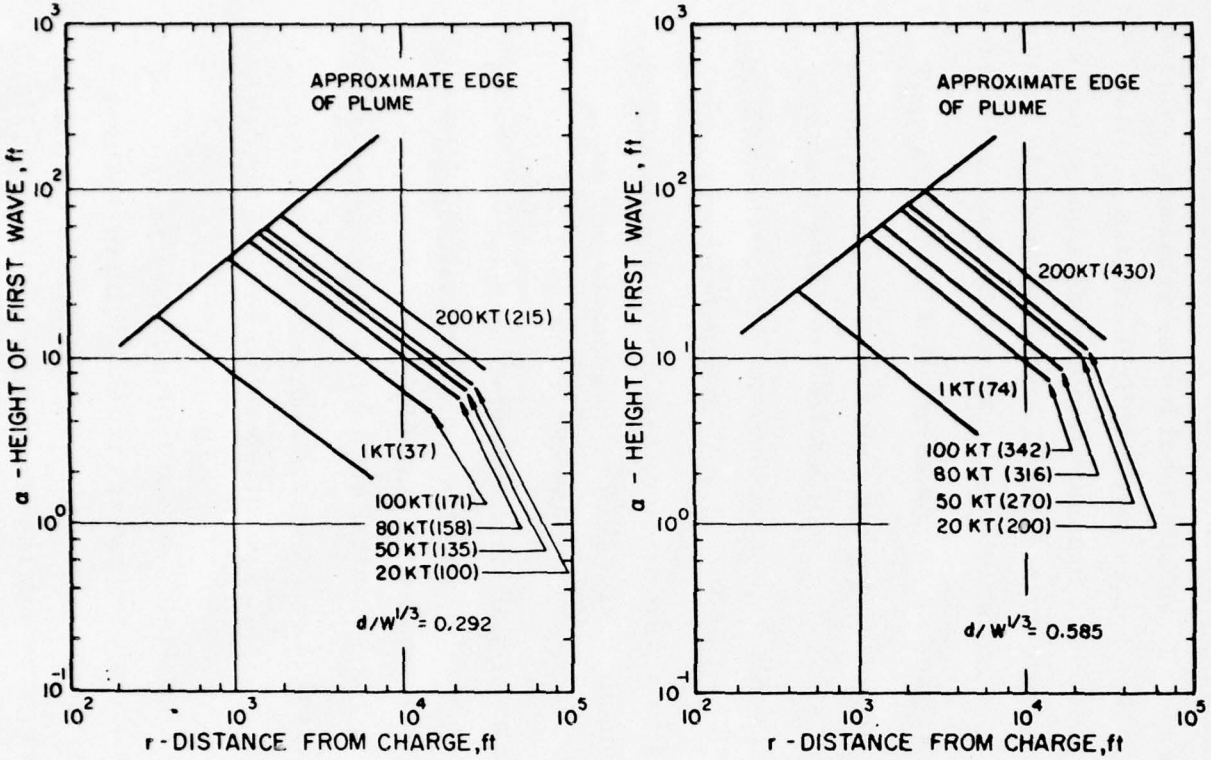

FIGURES IN PARENTHESES ARE ACTUAL WATER DEPTHS IN FEET FOR SPECIFIED YIELDS
ORIGINAL DATA UPON WHICH THESE CURVES ARE BASED EXHIBITED A SCATTER OF APPROXIMATELY ± 30% STANDARD DEVIATION OF A SINGLE OBSERVATION

Figure 2

Variation of wave height with distance

for various yields

charge at surface (Z = 0) $d/W^{1/3}$ = 0.292 and 0.585

4. RECOMMENDATIONS

There is a considerable lack of experimental data and theoretical work on water waves generated by shallow water explosions. However, from the extensive knowledge gained from studies of deep water explosions and the available data on shallow water explosions, a well defined program can be formulated which should lead to reliable prediction techniques in an efficient manner. The following problems and experimental tests are recommended for future consideration.

1. The data of this test series should be analyzed to determine

   a) $\eta_{max} r$ and T_{max} where wave envelopes still appear similar to deep water explosions

   b) The relationship of envelope amplitude with distance of the measurement station (in $\eta_{max} \propto \frac{1}{r}$).

   c) The energy partitioned to water waves as a function of water depth and submergence depth. This should be compared to that for deep water explosions.

   d) The comparison between these field tests and the various mathematical models presented in the Appendix. The theoretical solution should be obtained by a numerical integration technique near the front of the wave train.

   e) Attempt to classify the type of wave train produced to values of the reduced water depth $d/W^{1/3}$.

2. Perform an experimental test to determine the extent to which the small amplitude theory is applicable. This can be accomplished by simply measuring the water waves produced by either a cylindrical elevation or depression of the water surface (or preferably a cylindrical depression surrounded by a lip) and performing measurements of the wave train at various stations at distances r in the range $2R \leq r \leq 20R$ (R being the radius of the deformation). These

measurements should be made for various water depths starting with $4\eta_o R^2 / d^3 \ll 1$ and gradually decreasing d. Comparisons can then be made directly with the theoretical solution to ascertain the range of applicability of the linear theory for small amplitude waves.

3. An extensive shallow water test series with one charge weight (small, 1/2 - 10 lbs TNT) is recommended covering the range $0.5 \leq d/W^{1/3} \leq 6.0$ with submergence depths from surface to bottom for each value of $d/W^{1/3}$. It is particularly important to obtain a well defined upper critical depth. One should obtain measurements at many stations in constant depth water and it might prove of considerable value to take stereo-photographs of the generation area to provide data on the initial velocity field, actual maximum cavity radius, plume development, and mass transport (base surge) in the generation area.

4. Upon preliminary analysis of the above data, or simultaneously, 4-10 other charge weights should be selected for measurements at pre-determined critical values of $d/W^{1/3}$ and z (especially at upper critical depth).

5. Upon completion of the above test series, extensive analysis of the data and further comparison with theory should result in a prediction technique similar to that for deep water with the initial conditions of the mathematical model evaluated to produce empirically derived wave train characteristics.

6. Subsequent large scale field tests should be conducted (charge weights in excess of 5,000 lbs TNT equivalent) to evaluate the prediction techniques developed and provide more data to increase the reliability of extrapolation techniques.

7. It is relatively clear that the primary concern arising from detonations in the range $0.6 \leq d/W^{1/3} \leq 6.0$ is from the damage

potential to surface and subsurface ship traffic on the continental shelf when the detonation is somewhere on the continental slope. This presents another problem in so far as reliable predictions are concerned. Namely, in accurately describing the wave environment on the shelf. The previous studies lead to reliable predictions in water of constant depth and in establishing the mathematical model for the wave generation mechanism. Present techniques being applied for the prediction of explosively produced water waves over a non-uniform bottom are not applicable to this situation because the stationary phase approximation is not valid and the theoretical computation of the dispersive characteristics of the wave train are highly questionable. The problem arises from the computation of, for example, two or even less than one wave in the first envelope because dispersion is retarded for the rapidly decreasing water depth. Further theoretical work without using the stationary phase approximation is recommended in this important area as well as small scale field tests with spherical TNT charges and a bottom modeled to represent a typical east coast situation. Perhaps later a large scale field test would be beneficial, but only subsequent to performance and evaluation from the small scale tests.

8. One consideration which should not be overlooked is the case of multiple explosions in a similar situation on the continental slope. If wave amplitudes can be increased by a factor of 2-4 from two detonations, it tremendously increases the utility of this concept due to the relatively non-critical item of charge placement (100 - 400 ft. relative to one another for weapons in the IMT class).

REFERENCES

1. "Effects of Explosions in Shallow Water," U.S. Corps of Eng., WES, Final Report, TM 2-406, AFSWP-452, April 1955

2. Whalin, R.W. and D. Divoky, "Water Waves Generated by Shallow Water Explosions (U)," National Engineering Science Company Report S-359, NCEL No. CR 67.018, Nov. 1965

APPENDIX MATHEMATICAL MODEL FOR WATER WAVES GENERATED BY EXPLOSIONS IN SHALLOW WATER

This section describes the mathematical formulation of the problem including its expected region of validity and the general solution. Various methods of representing the generation mechanism are presented along with several sample calculations.

A.1 Theoretical Formulation

The general formulation of the mathematical model to be applied to the problem appears in the works of Kajiura (Ref. 1) and Whalin (Refs. 2 and 3). This formulation is based on the linear theory of surface waves in an inviscid, incompressible fluid of constant depth. The source of disturbance can be either a surface deformation, bottom deformation, or initial velocity field which is not necessarily symmetric. However, in the problem under consideration, the source is assumed to be either a stationary surface deformation or a time-dependent deformation which, in this case, is equivalent to assuming an initial velocity distribution.

The kinematic and dynamic conditions at the free surface are

$$\varphi_z = \eta_t, \qquad z = 0 \tag{1}$$

$$\varphi_t = -\eta - P, \quad z = 0 \tag{2}$$

and the bottom condition is

$$\varphi_z = 0, \qquad z = -1 \tag{3}$$

The time-dependent Green's Function G is a solution of the Laplace equation

$$\nabla^2 G = 0, \qquad 0 > z > -1, \qquad t \geq \tau \tag{4}$$

satisfying the free surface condition

$$G_{tt} + G_z = 0, \quad z = 0 \tag{5}$$

and the bottom condition

$$G_z = 0, \qquad z = -1 \tag{6}$$

It is required that G, G_x, G_y, G_z, G_t, G_{tx}, G_{ty}, and G_{tz} be uniformly bounded for every t at $x, y \to \infty$ and that $(G - 1/\rho)$ be bounded at (x_o, y_o, z_o) where

$$\rho^2 = (x - x_o)^2 + (y - y_o)^2 + (z - z_o)^2 \tag{7}$$

At time $t = \tau$, it is assumed that

$$G = G_t = 0, \qquad z = 0 \tag{8}$$

G is determined uniquely from the above equation and conditions.

The Green's function for the case of three-dimensional motion in a fluid of finite depth is

$$\begin{aligned} G(x_o, y_o, z_o; \tau | x, y, z, t) = \int_0^\infty \frac{J_o(m\bar{r})}{\cosh m} \Big[& \sinh m \{1 - |z - z_o|\} \\ & - \sinh m \{1 + (z + z_o)\} + \frac{1}{\gamma^2} \\ & \cdot \{1 - \cosh \gamma (t - \tau)\} \frac{m}{\cosh m} \\ & \cdot \cosh m (1 + z) \cosh m (1 + z_o) \Big] dm, \\ & 0 > z, \quad z_o > -1 \end{aligned} \tag{9}$$

where

$$\bar{r}^2 = (x - x_o)^2 + (y - y_o)^2 \tag{10}$$

and

$$\gamma^2 = m \tanh m$$

Assuming the disturbance in the present case to be that of an initial surface deformation or an initial velocity distribution, the solution for the wave amplitude becomes

$$\eta = \frac{1}{4\pi} \iint_S \left(G_t \varphi_{z_o} - G_{\tau t} \eta \right)_{t = 0} dS, \; z_o = 0, \; z = 0 \tag{11}$$

A. 2 Initial Conditions and Solutions

The wave generation mechanism of an explosion in shallow water is certainly an extremely complicated hydrodynamic phenomenon. However, for the purpose of this investigation, two classes of initial conditions were assumed:

a) A stationary axially symmetric surface deformation

b) An axially symmetric initial velocity field (prescribed such that it will approximately generate a desired surface deformation at a small time τ^* after the detonation)

Table I shows the various types of initial deformation considered; Table II shows the zero order Hankel Transform of the deformation, and Figs. 1a and 1b are illustrations of the deformations.

TABLE I

Initial Deformations Simulating an Explosion in Shallow Water

1.	$\eta = -d$	$r_o \leq R$
	$\eta = 0$	$r_o > R$
2.	$\eta = -d$	$0 \leq r_o \leq R_1$
	$\eta = -\frac{R^2 d}{R^2 - R_1^2}\left(1 - \frac{r^2}{R^2}\right)$	$R_1 \leq r_o \leq R$
	$\eta = 0$	$r_o \geq R$
3.	$\eta = -d$	$r_o \geq R$
	$\eta = -\frac{R^2 d}{R^2 - R_1^2}\left(1 - \frac{r^2}{R^2}\right)$	$R_1 \leq r_o \leq R$
	$\eta = \frac{3d}{16}\frac{R^2 + R_1^2}{R_2(R_2 - R_1)}\left\{1 - \left(\frac{r_o - R_2}{R - R_2}\right)^2\right\}$	$R \leq r_o \leq 2R_2 - R$
	$\eta = 0$	$r_o \geq 2R_2 - R$
4.	$\eta = -d$	$r_o < R$
	$\eta = \frac{R^2 d}{4R_2(R_2 - R)}$	$R < r_o < 2R_2 - R$
	$\eta = 0$	$r_o > 2R_2 - R$

TABLE I

Initial Deformations Simulating
an Explosion in Shallow Water
(Continued)

5.	$\eta = -d$	$r_o < R$
	$\eta = \frac{3}{8} \frac{R^2 d}{R_2 (R_2 - R)} \left\{ 1 - \left(\frac{r_o - R_2}{R_2 - R} \right)^2 \right\}$	$R \le r_o \le 2R_2 - R$
	$\eta = 0$	$r_o \ge 2R_2 - R$
6.	$\eta = -d$	$r_o \le R_1$
	$\eta = -\frac{R^2 d}{R^2 - R_1^2} \left(1 - \frac{r^2}{R^2} \right)$	$R_1 \le r_o \le \left(R^2 + \sqrt{R^4 - R_1^4} \right)^{1/2}$
	$\eta = 0$	$r_o > \left(R^2 + \sqrt{R^4 - R_1^4} \right)^{1/2}$
7.	$\eta = -d$	$r_o \le R_1$
	$\eta = Ar^4 + Br^2 + C$	$R_1 \le r_o \le R_3$
	$\eta = 0$	$r_o \ge R_3$
	$A = \frac{-d}{(R^2 - R_1^2)(R_3^2 - R_1^2)}$	$C = \frac{-d R^2 R_3^2}{(R^2 - R_1^2)(R_3^2 - R_1^2)}$
	$B = \frac{d(R^2 + R_3^2)}{(R^2 - R_1^2)(R_3^2 - R_1^2)}$	$R_3 = \frac{1}{\sqrt{2}} \left\{ 3R^2 - R_1^2 + \sqrt{9R^4 + 6R^2 R_1^2 - 15R_1^4} \right\}^{1/2}$

TABLE II

Zero Order Hankel Transform of the

Initial Deformations

1. $\overline{\eta_o}(m) = - d \frac{R}{m} J_1(m R)$

2. $\overline{\eta_o}(m) = \frac{2d}{m^2\left(R^2 - R_1^2\right)} \left\{R_1^2 J_2\left(m R_1\right) - R^2 J_2(m R)\right\}$

3. $\overline{\eta_o}(m) = - J_o(m R) \frac{3d}{8} \frac{R}{m^2} \frac{R^2 + R_1^2}{\left(R_2 - R\right)^3}$

$$+ J_o\left(2m R_2 - m R\right) \frac{3d}{8} \frac{2R_2 - R}{m^2} \frac{R^2 + R_1^2}{\left(R_2 - R\right)^3}$$

$$+ J_2\left(m R_1\right) \frac{2d R_1^2}{m^2\left(R^2 - R_1^2\right)}$$

$$- J_2(m R) \left\{\frac{2d R^2}{m^2\left(R^2 - R_1^2\right)} + \frac{3d}{8} \frac{R^2}{m^2} \frac{R^2 + R_1^2}{R_2\left(R_2 - R\right)^3}\right\}$$

$$+ J_2\left(2m R_2 - m R\right) \frac{3d}{8} \frac{\left(2R_2 - R\right)^2}{m^2} \frac{R^2 + R_1^2}{R_2\left(R_2 - R\right)^3}$$

$$+ \frac{3d}{8m^3} \frac{R^2 + R_1^2}{\left(R_2 - R\right)^3} \left\{\int_0^{m R} J_o(t)\, dt - \int_0^{2m R_2 - m R} J_o(t)\, dt\right\}$$

TABLE II

Zero Order Hankel Transform of the

Initial Deformations

(Continued)

$$4.\quad \overline{\eta_o}(m) = -J_1(mR)\frac{Rd}{m}\left\{1+\frac{R^2}{4R_2(R_2-R)}\right\} + J_1\left(2mR_2 - mR\right)\frac{R^2 d(2R_2-R)}{4mR_2(R_2-R)}$$

$$5.\quad \overline{\eta_o}(m) = -J_o(mR)\frac{3}{4}\frac{R^3 d}{m^2(R_2-R)^3} + J_o\left(2mR_2 - mR\right)\frac{3}{4}\frac{R^2 d(2R_2-R)}{m^2(R_2-R)^3} - J_1(mR)\frac{Rd}{m}$$

$$- J_2(mR)\frac{3}{4}\frac{R^4 d}{m^2 R_2(R_2-R)^3} + J_2\left(2mR_2 - mR\right)\frac{3}{4}\frac{R^2 d(2R_2-R)^2}{m^2 R_2(R_2-R)^3}$$

$$+ \frac{3}{4m^3}\frac{R^2 d}{(R_2-R)^3}\left\{\int_0^{mR} J_o(t),dt - \int_0^{2mR_2 - mR} J_o(t)\,dt\right\}$$

TABLE II

Zero Order Hankel Transform of the
Initial Deformations
(Continued)

$$6.\quad \overline{\eta_o}(m) = J_1\left(m\sqrt{R^2 + \sqrt{R^4 - R_1^4}}\right)\frac{d\left(R^4 - R_1^4\right)^{1/2}}{m\left(R^2 - R_1^2\right)}\left(R^2 + \sqrt{R^4 - R_1^4}\right)^{1/2}$$

$$+ J_2\left(m R_2\right)\frac{2d R_1^2}{m^2\left(R^2 - R_1^2\right)}$$

$$- J_2\left(m\sqrt{R^2 + \sqrt{R^4 - R_1^4}}\right)\frac{2d}{m^2\left(R^2 - R_1^2\right)}\left(R^2 + \sqrt{R^4 - R_1^4}\right)$$

$$7.\quad \overline{\eta_o}(m) = \frac{R_1^2}{m^2} J_2\left(m R_1\right)\left\{4 A R_1^2 + 2B\right\}$$

$$- \frac{R_3^2}{m^2} J_2\left(m R_3\right)\left\{4 A R_3^2 + 2B\right\}$$

$$- \frac{R_1^3}{m^3} J_3\left(m R_1\right)\ 8 A + \frac{R_3^3}{m^3} J_3\left(m R_3\right)\ 8 A$$

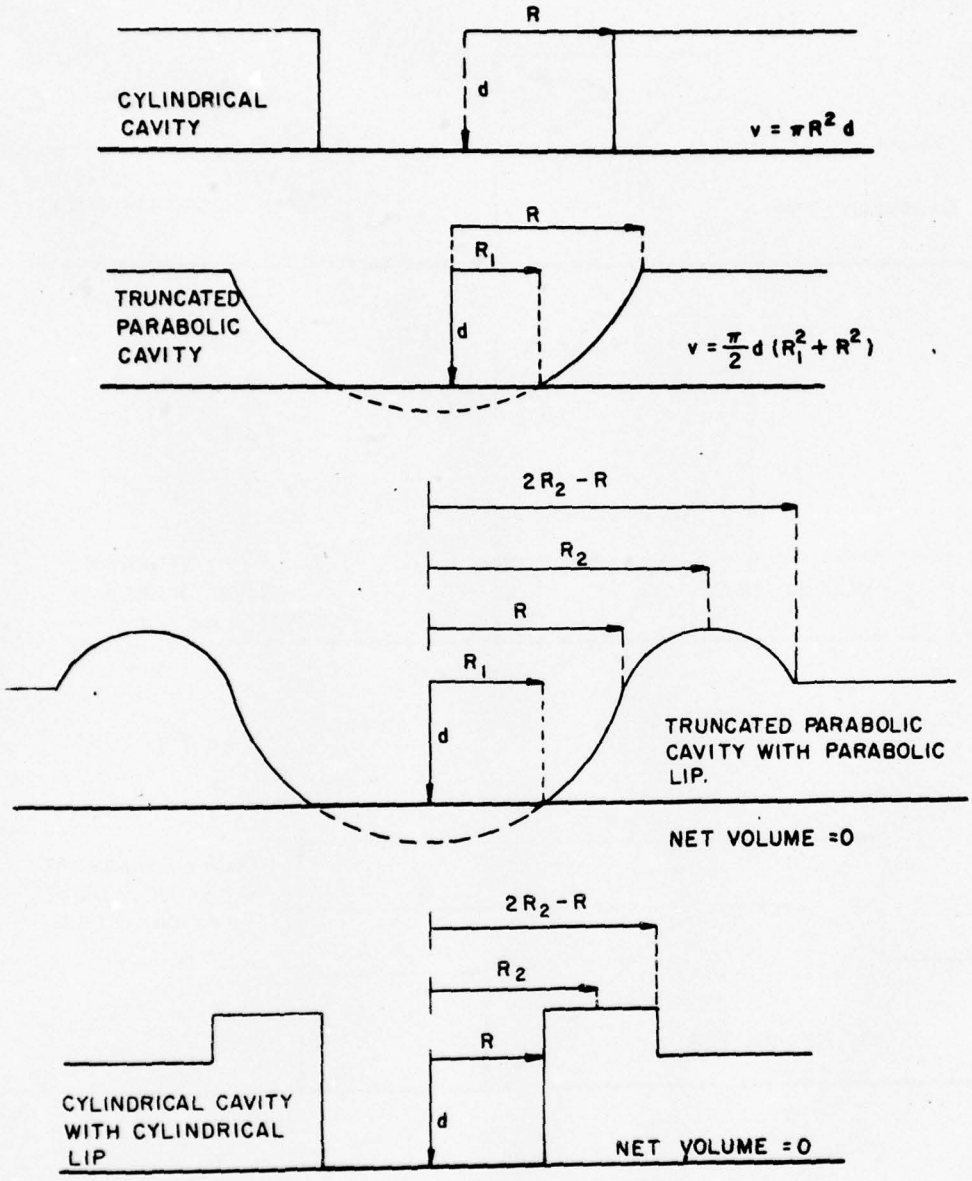

Figure 1a

Initial deformations simulating a shallow water detonation

PA-3-10202

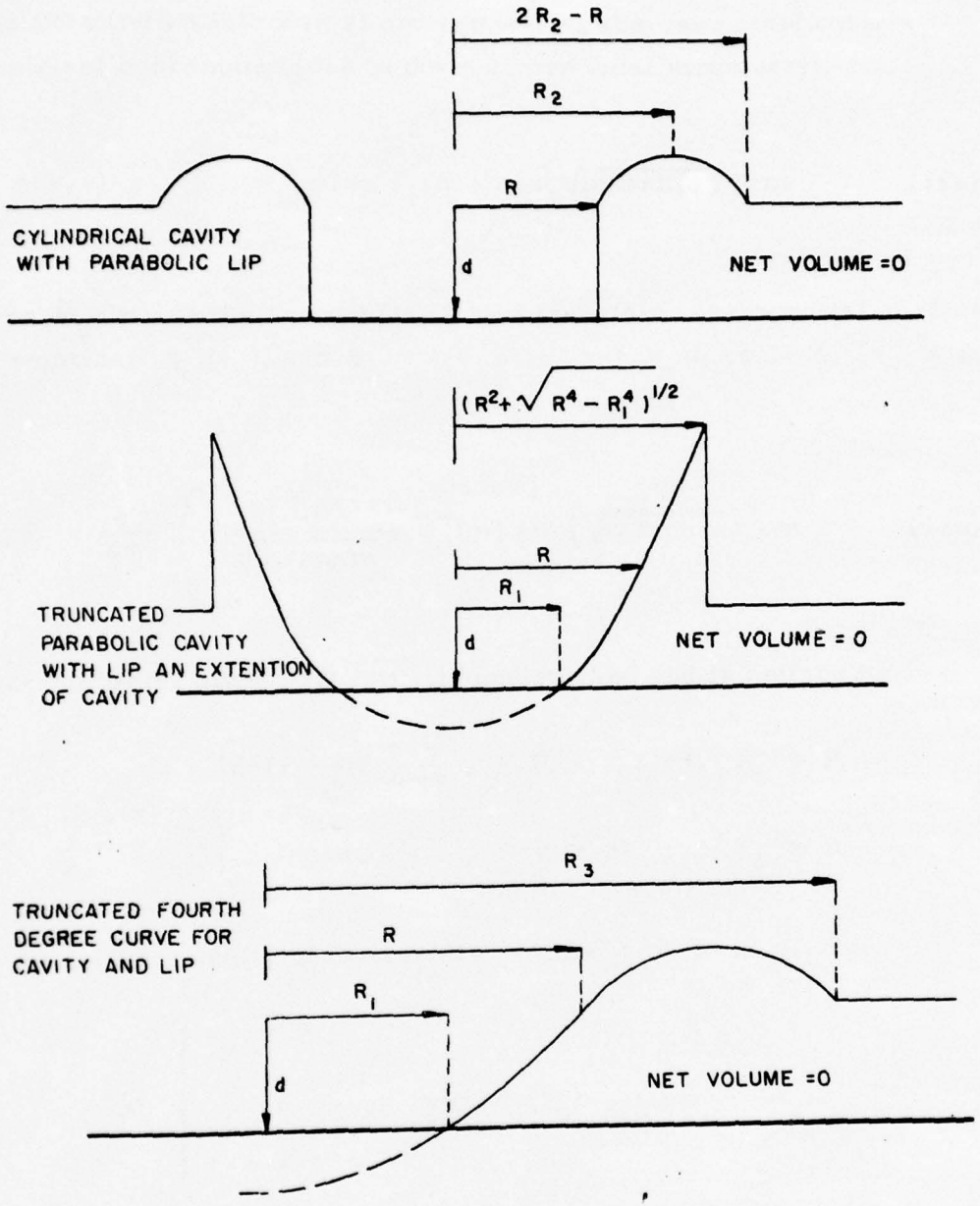

Figure 1b

Initial deformations simulating a shallow water detonation

PA-3-10203

Upon substitution into Eq. 11 and expressing the wave amplitude in cylindrical coordinates (due to the assumed axial symmetry),

$$\eta(r, t) = -\int_0^\infty \overline{\eta_o}(m)\, m\, J_o(m\, r) \cos\left(\sqrt{m \tanh m}\, t\right) dm \qquad (12a)$$

where $\overline{\eta}_o(m)$ is the zero order Hankel transform of the initial surface deformation, $\eta_o(r_o)$, and $\varphi_{z_o} = 0$ at $\tau = t = 0$; $z = 0$; $z_o = 0$, or

$$\eta(r, t) = \frac{\pi}{2\tau^*} \int_0^\infty \frac{m\, J_o(m\, r)}{\sqrt{m \tanh m}}\, \overline{\eta_o}(m) \sin\left(\sqrt{m \tanh m}\, t\right) dm \qquad (12b)$$

where the water surface is initially undisturbed and is defined by

$$\eta_o(r_o, \tau) = \begin{cases} \eta_o(r_o) \sin\frac{\pi}{2}\frac{\tau}{\tau^*}, & 0 \le \tau \le \tau^*,\ r_o \le R \\ 0, & \tau > \tau^*,\ r_o > R \end{cases}$$

and the initial velocity of the surface at time $\tau = 0$ is

$$\varphi_{z_o}\Big|_{\substack{z_o = 0 \\ z = 0 \\ \tau = t = 0}} = \frac{\tau}{2\tau^*}\, \eta_o(r_o)$$

The usual technique of evaluating the above integral is to apply the method of stationary phase for a large distance r from the detonation. However, in the case under consideration, the cavity reaches to the bottom and the deformation is not small in either depth or extent when compared to the water depth. Furthermore, the dimensionless wave

number in the areas of interest is relatively small ($0 \leq m \leq 3/2$). However, the use of the method of stationary phase will be accurate within a few percent provided that the wave train is computed at distances r which are greater than five times the assumed cavity radius, and it is realized that the computation for values of $m < 0.4$ is successively more in error. A precise method of evaluating this integral (such as Whalin, Ref. 4) will result in an elevation of the water surface for all times $t > 0$ due to the assumption of an incompressible fluid and the fact that the surface deformation creates a velocity field throughout the fluid instantaneously.

In order to evaluate the applicability of this linear theory, it is sufficient to use the method of stationary phase for evaluating the integral in Eq. 12. However, in formulating an actual prediction method, relating initial deformations and velocity fields to W, d, and Z, and evaluating the accuracy of the method, the integral should be computed by other methods for certain regions in both space and time.

Upon evaluation of Eq. 12 by the method of stationary phase, the expression for the wave amplitude becomes

$$\eta(r, t) = \frac{1}{r} \sqrt{\frac{\Phi(m)}{-\Phi''(m)}}\, \overline{\eta_o}(m) \cos\left(m r - \sqrt{m \tanh m}\, t\right) \qquad (13a)$$

for a stationary initial surface deformation and

$$\eta(r, t) = \frac{\pi}{2\tau^*} \frac{\overline{\eta_o}(m)}{r \sqrt{\tanh m}} \sqrt{\frac{\Phi(m)}{-\Phi''(m)}} \sin\left(m r - \sqrt{m \tanh m}\, t\right) \qquad (13b)$$

for a time-dependent initial surface deformation of the type given in Eq. 12b where

$$\Phi(m) \equiv \frac{1}{2}\sqrt{\frac{\tanh m}{m}} + \frac{1}{2\cosh^2 m}\sqrt{\frac{m}{\tanh m}} = \frac{r}{t} \times \frac{1}{\sqrt{gd}} \qquad (14)$$

One example of each of the seven mathematical models shown in Fig. 1 was calculated, first assuming the stationary initial deformation, and second assuming an initial velocity field with $\tau^* = 4.35$ (chosen for convenience in the numerical calculation). The initial conditions used are shown in Table III and were chosen to approximate conditions of one of the WES 1955 test series in very shallow water.

TABLE III

Model	d(ft)	R_1	R	R_2	R_3
I	0.927	----	2.60	----	----
II	0.927	2.60	3.96	----	----
III	0.927	2.60	3.96	5.66	----
IV	0.927	----	2.60	3.66	----
V	0.927	----	2.60	4.03	----
VI	0.927	2.60	3.96	----	----
VIII	0.927	2.60	4.39	----	7.41

The first few waves of each of the wave trains generated is shown in Figs. 2 through 15. The figures which illustrate a time-dependent deformation show waves of an amplitude which is impossible in some cases. The reason for this is a poor choice for τ^* and the fact that the linear theory may not be applicable for prediction purposes unless physically unreasonable initial conditions are assumed. At any rate, the qualitative features of the wave trains can be ascertained and the

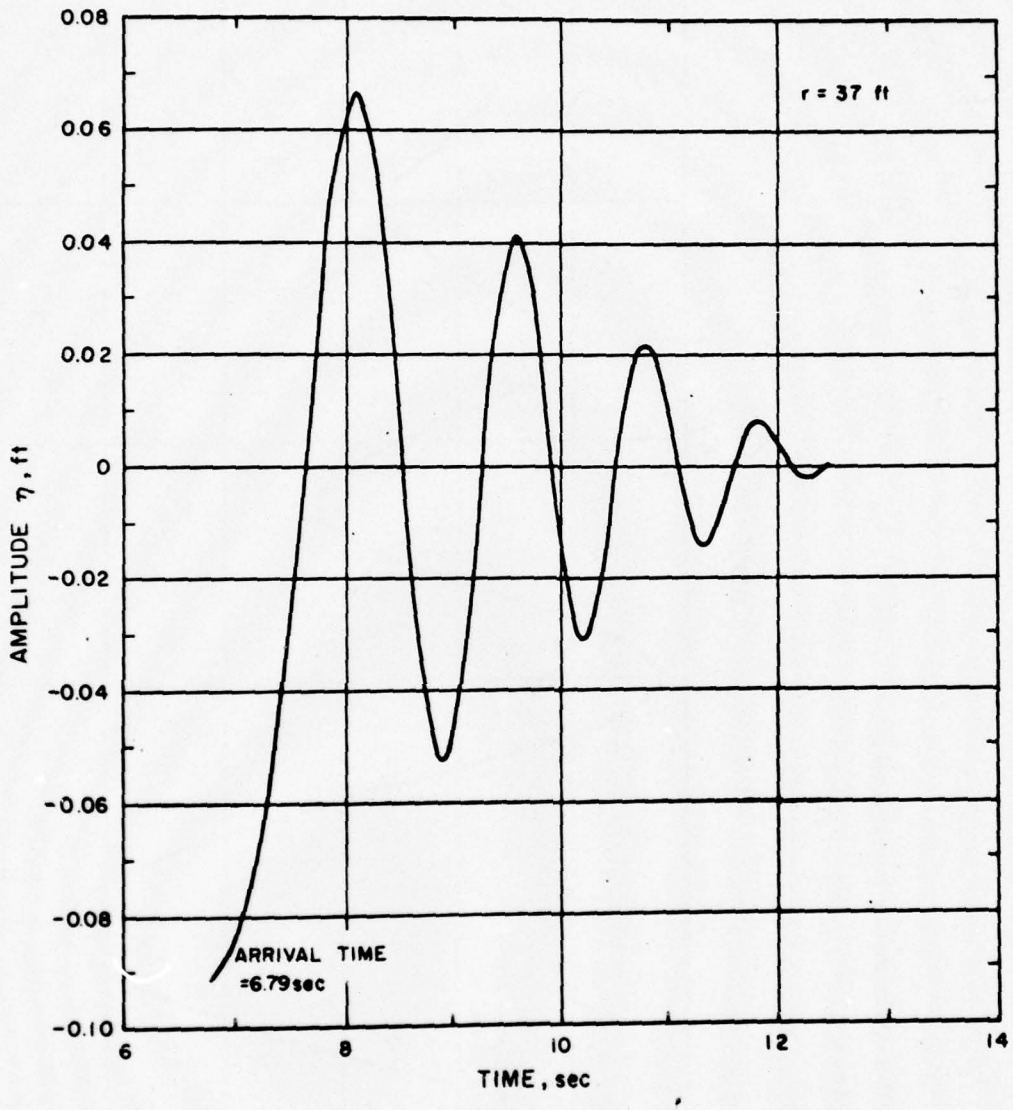

Figure 2
Stationary initial surface deformation, cylindrical cavity

PA-3-10204

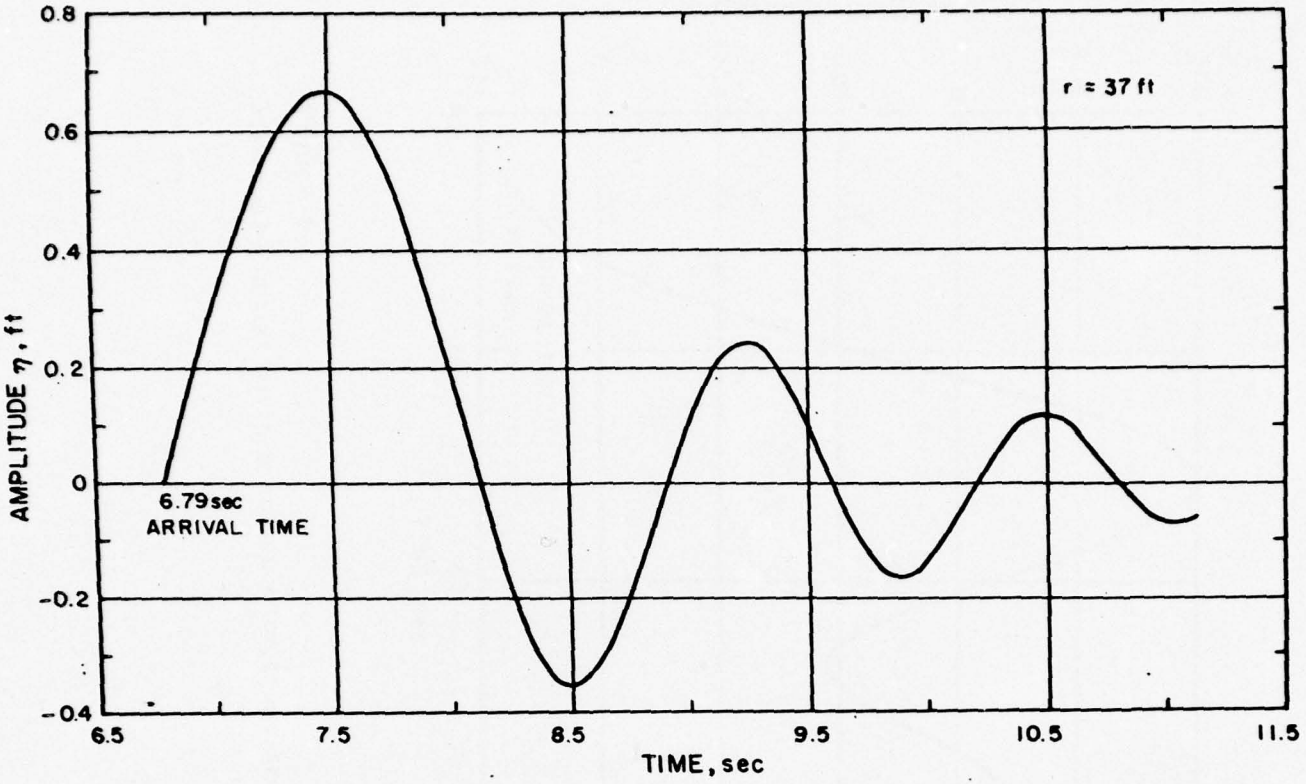

Figure 3

Time-dependent initial surface deformation, cylindrical cavity

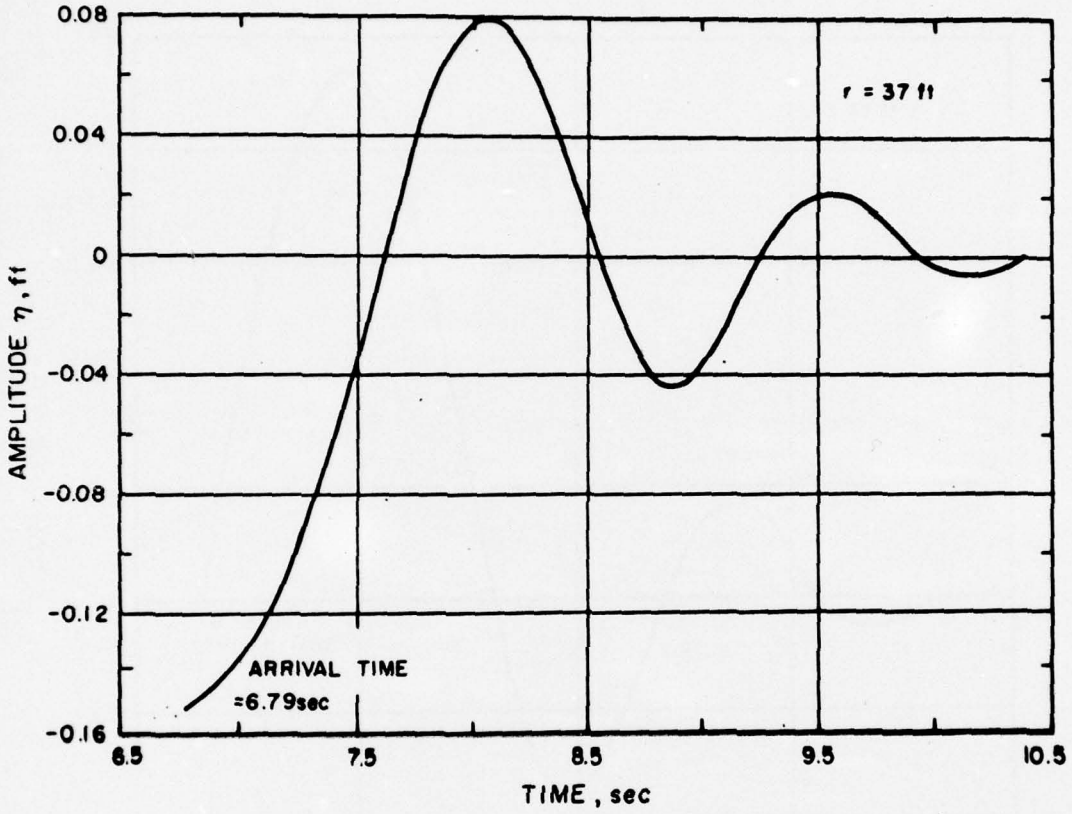

Figure 4
Stationary initial surface deformation, truncated parabola

PA-3-10206

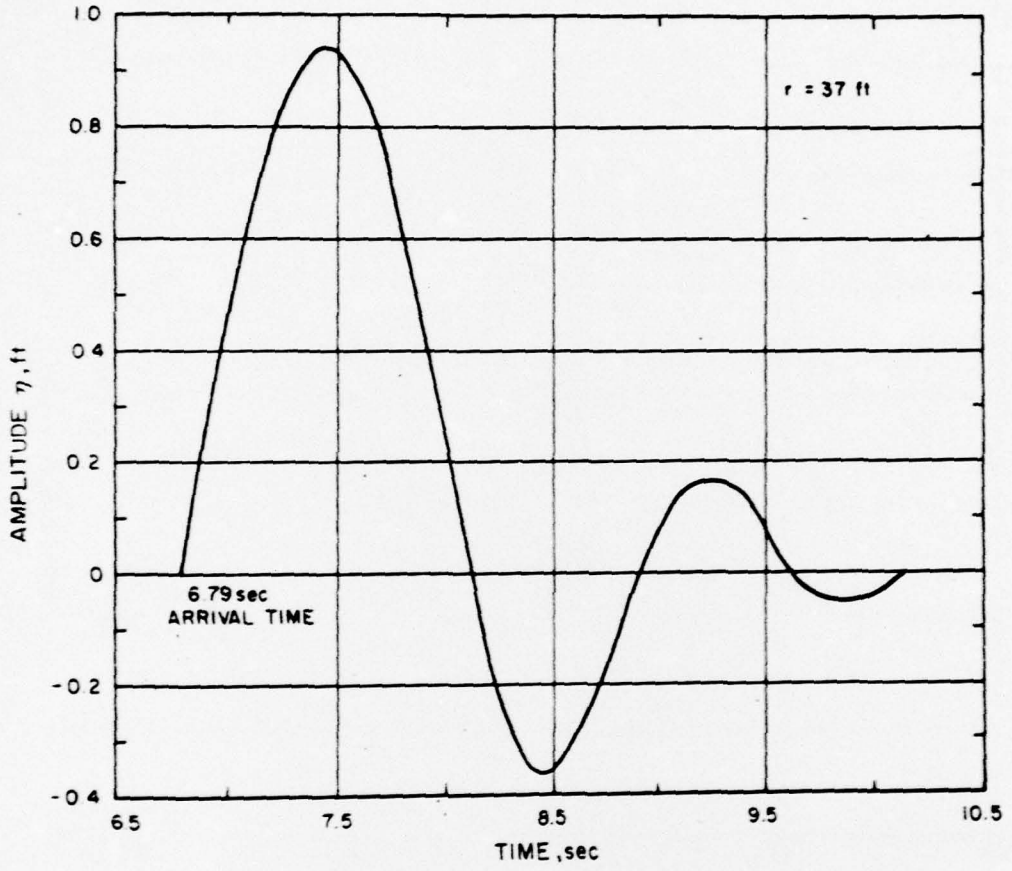

Figure 5

Time-dependent initial surface deformation, truncated parabola

PA-3-10207

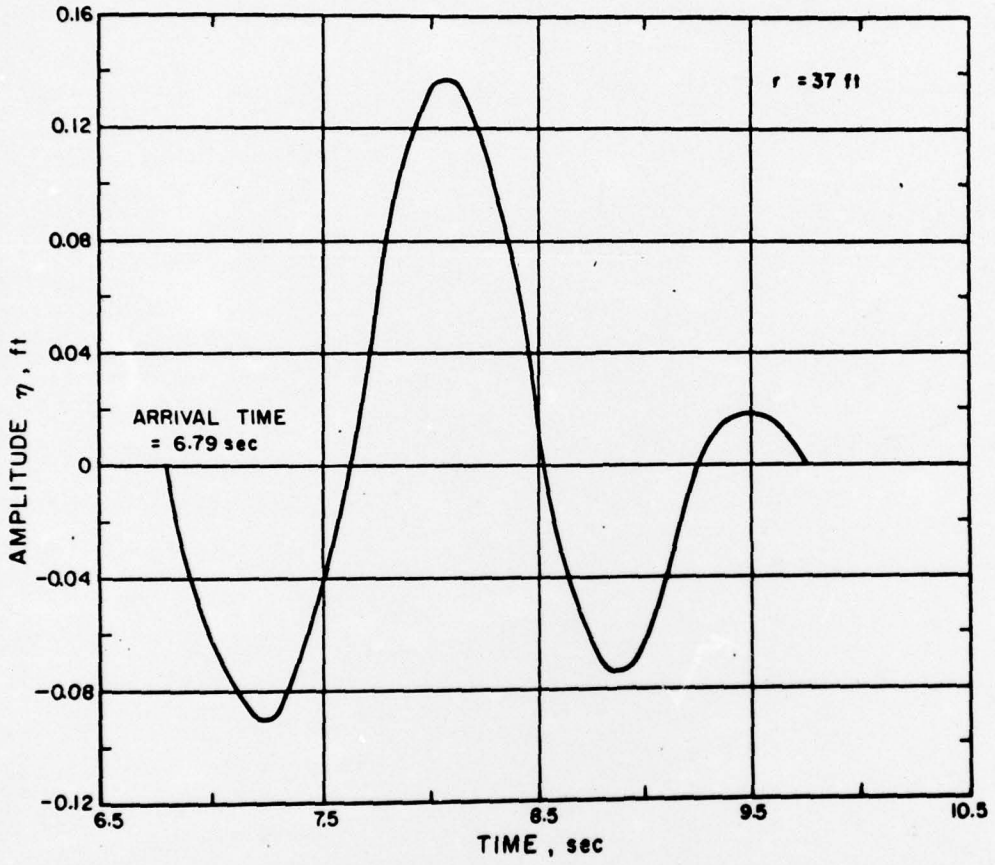

Figure 6
Stationary initial surface deformation, truncated parabolic cavity with a parabolic lip

PA-3-10208

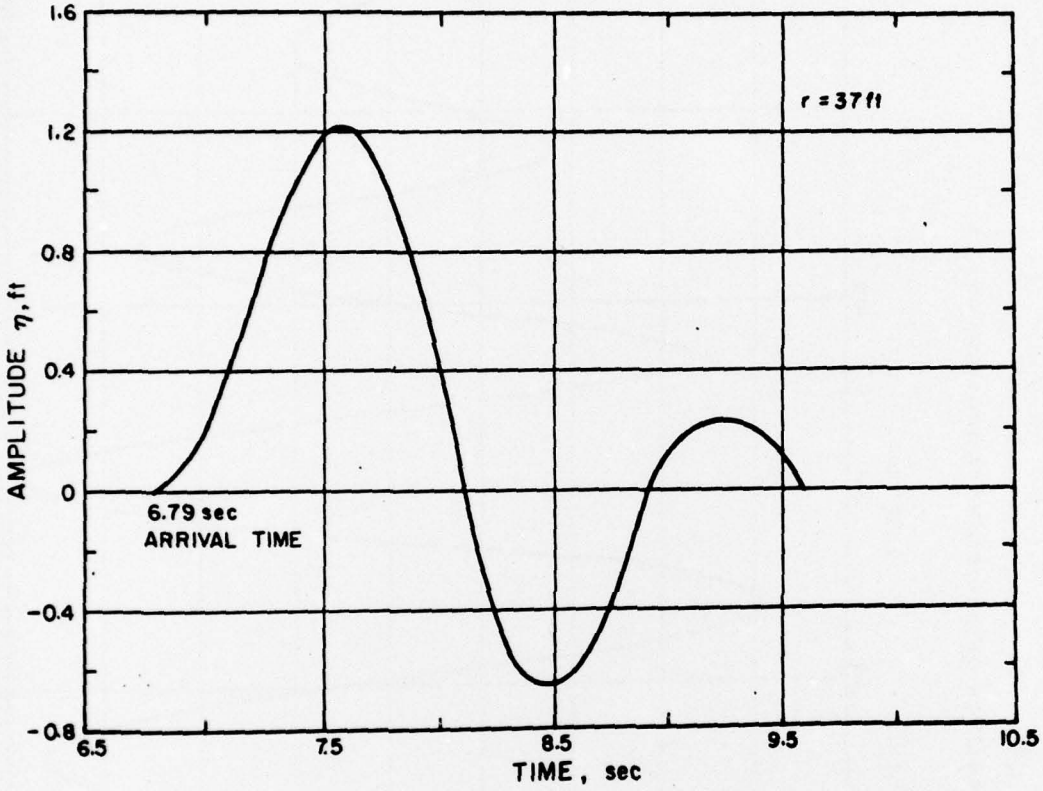

Figure 7
Time-dependent initial surface deformation, truncated parabolic cavity with a parabolic lip

PA-3-10209

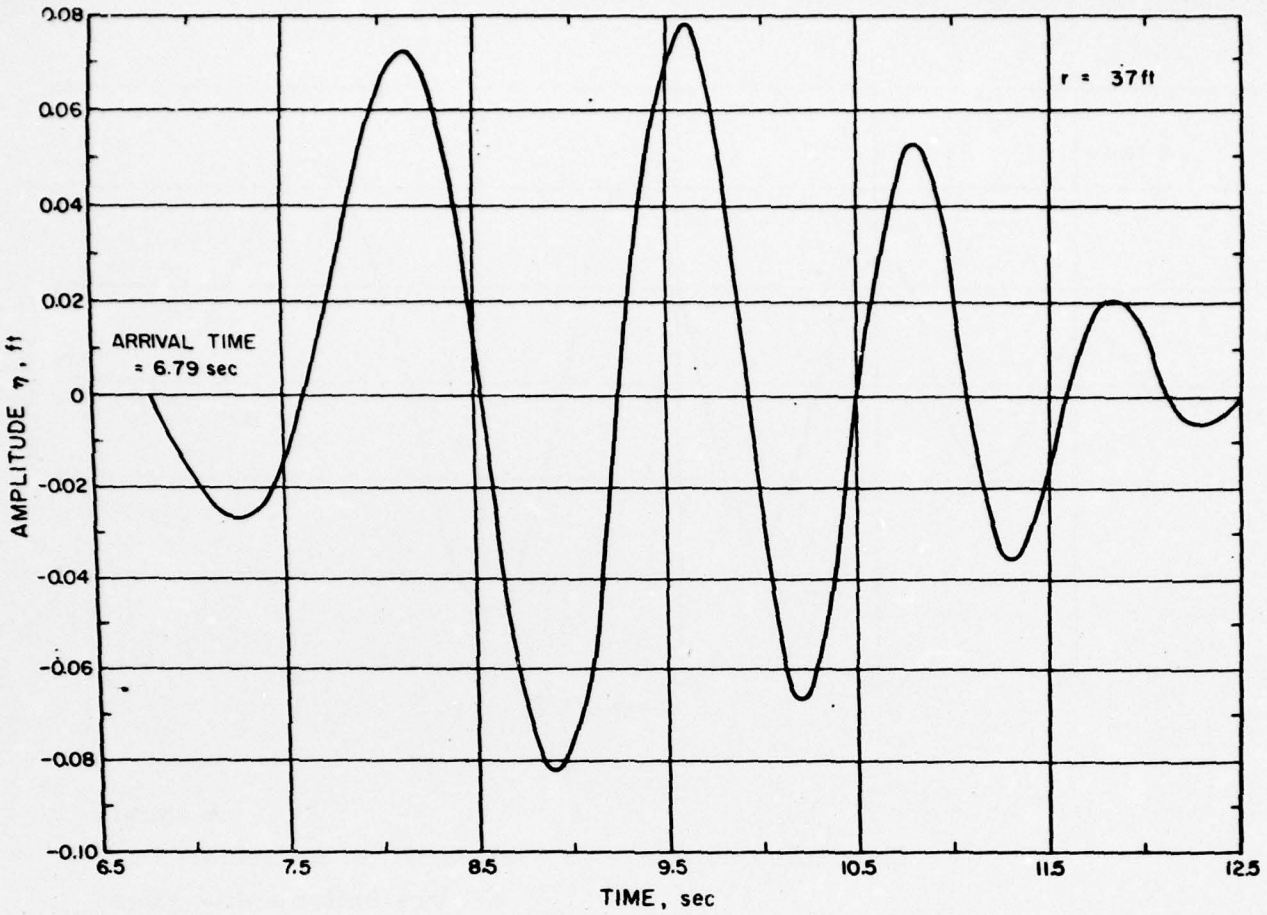

Figure 8

Stationary initial surface deformation, cylindrical cavity with a cylindrical lip

PA-3-10210

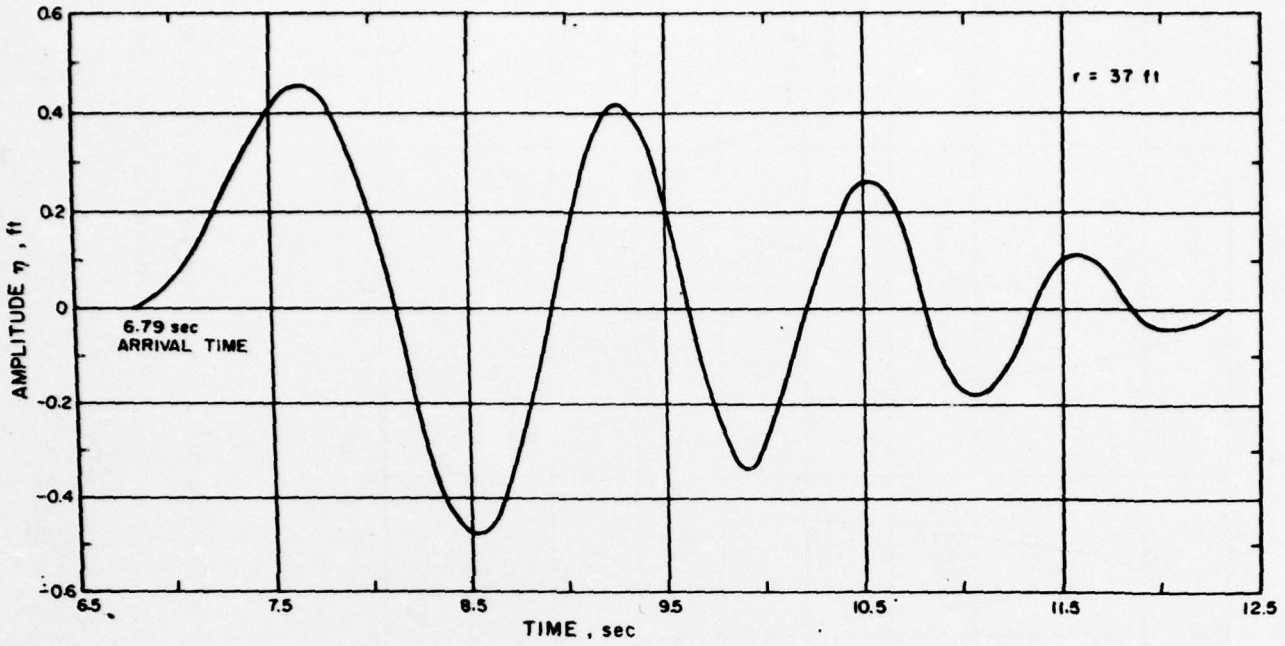

Figure 9

Time-dependent initial surface deformation, cylindrical cavity with a cylindrical lip

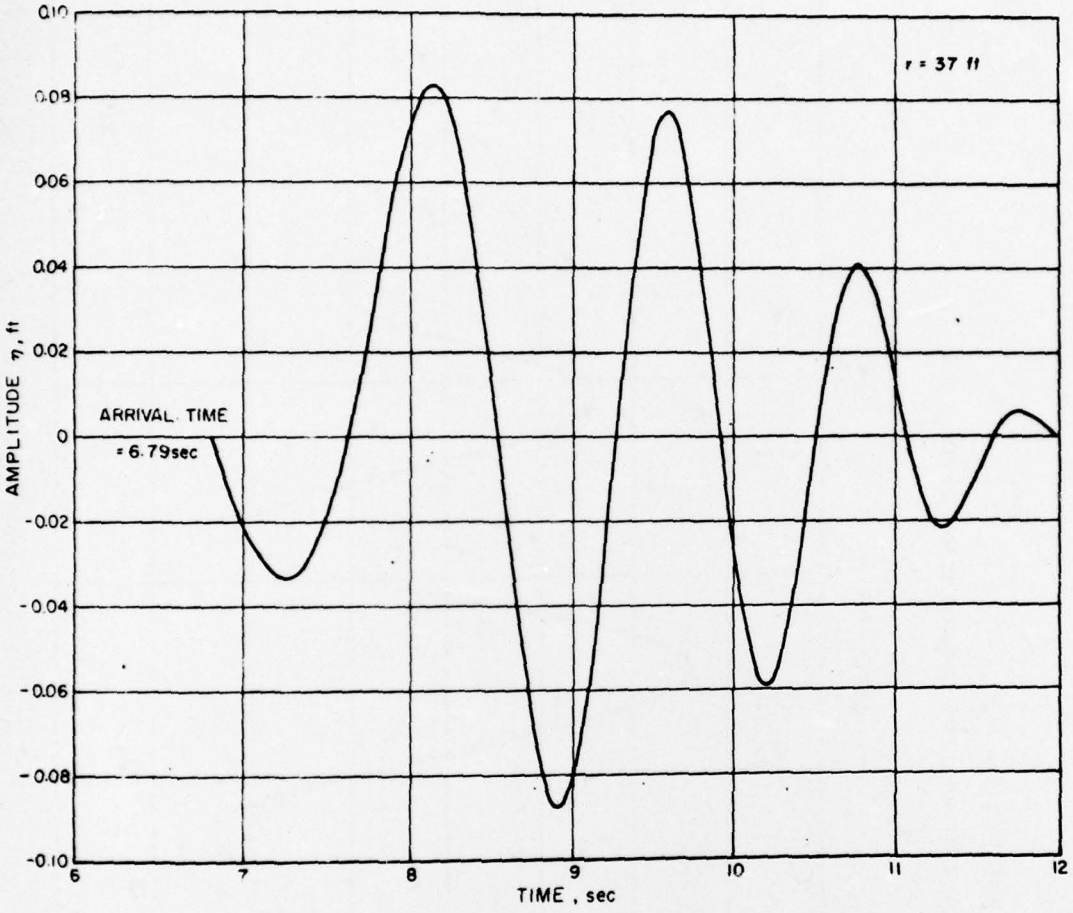

Figure 10
Stationary initial surface deformation, cylindrical cavity with a parabolic lip

PA-3-10212

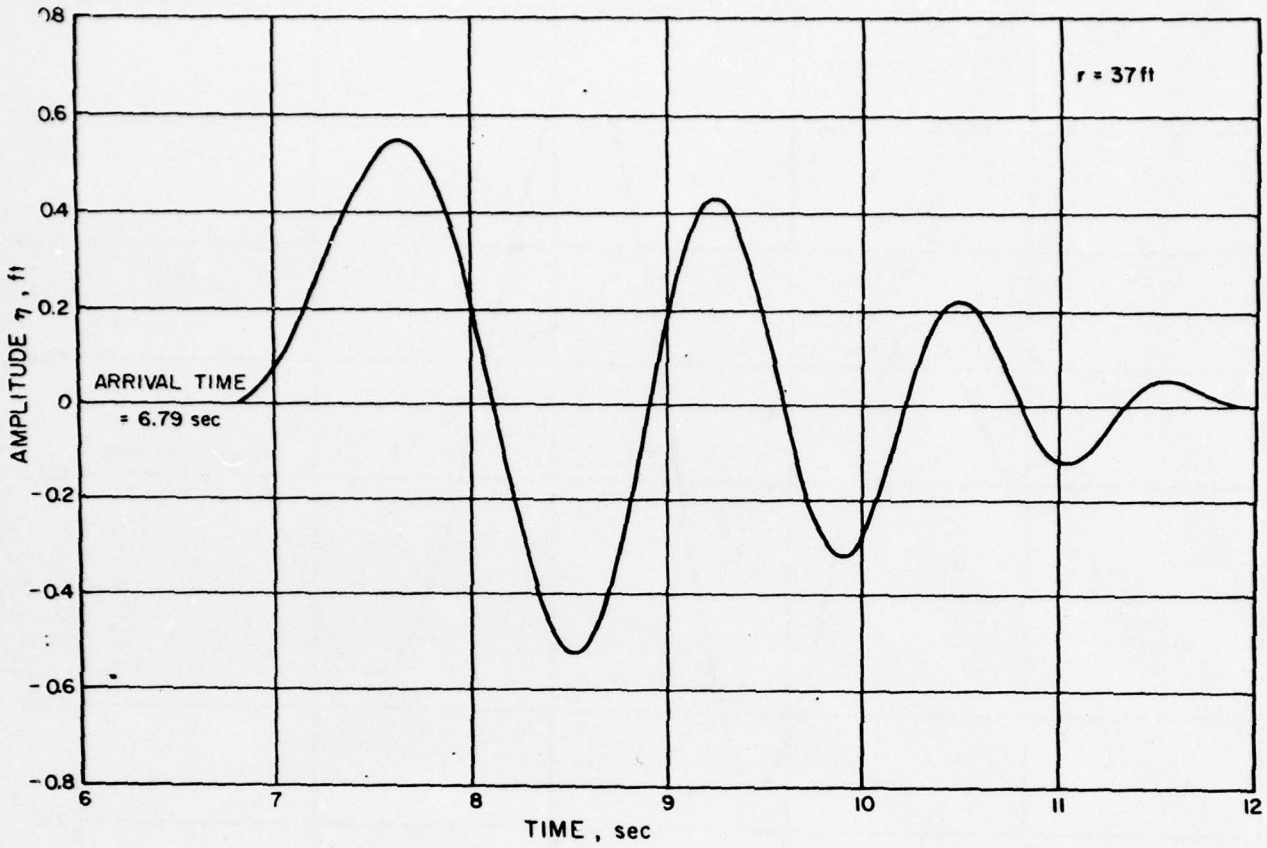

Figure 11

Time-dependent initial surface deformation, cylindrical cavity with a parabolic lip

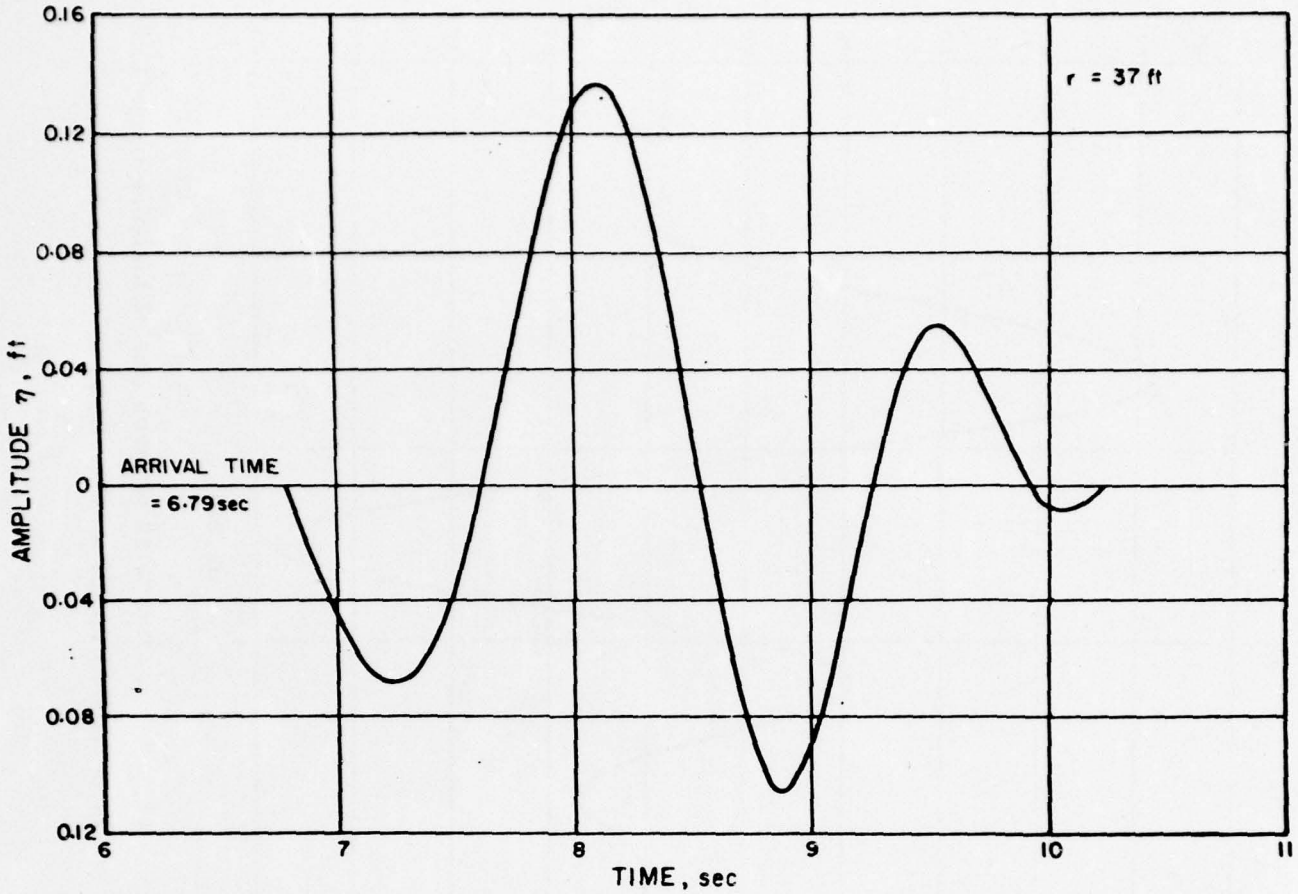

Figure 12
Stationary initial surface deformation, truncated parabolic cavity with a lip an extension of the cavity

PA-3-10214

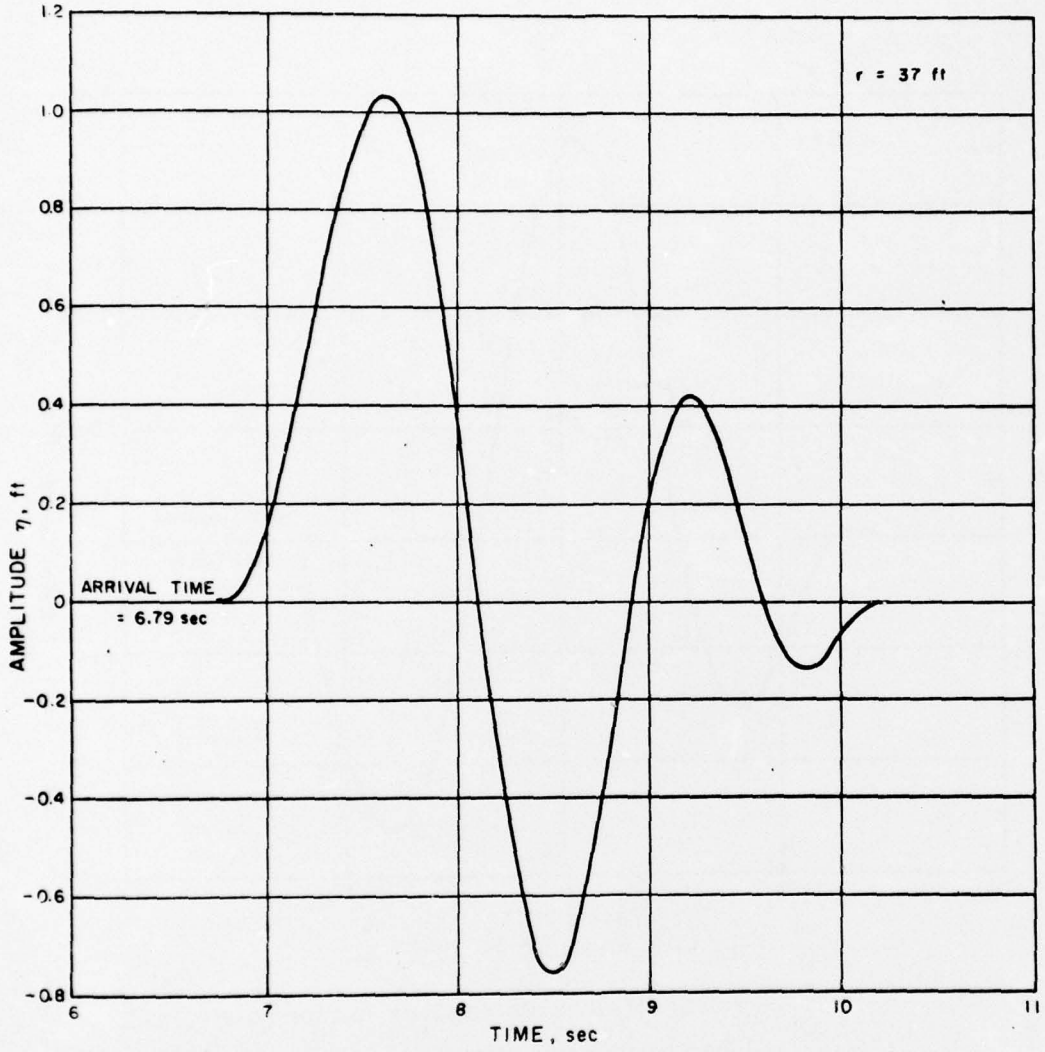

Figure 13

Time-dependent initial surface deformation,

Truncated parabolic cavity with a lip an extension of the cavity

PA-3-10215

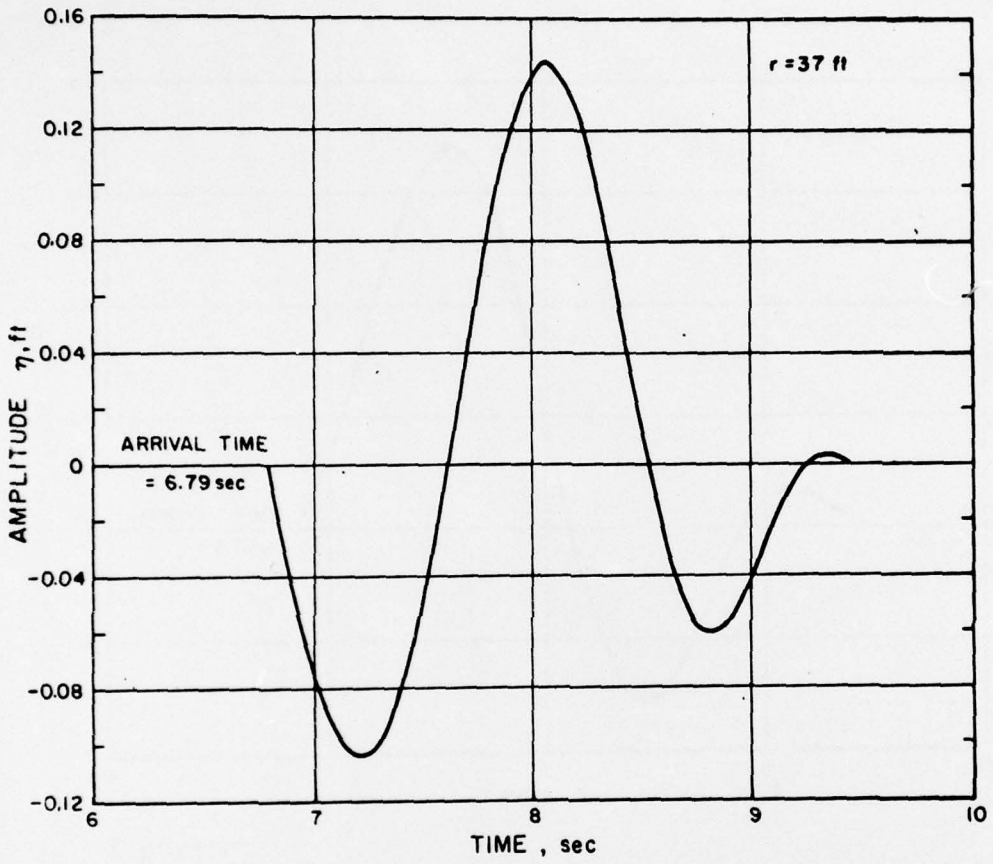

Figure 14
Stationary initial surface deformation,
truncated 4th degree curve for cavity and lip

PA-3-10216

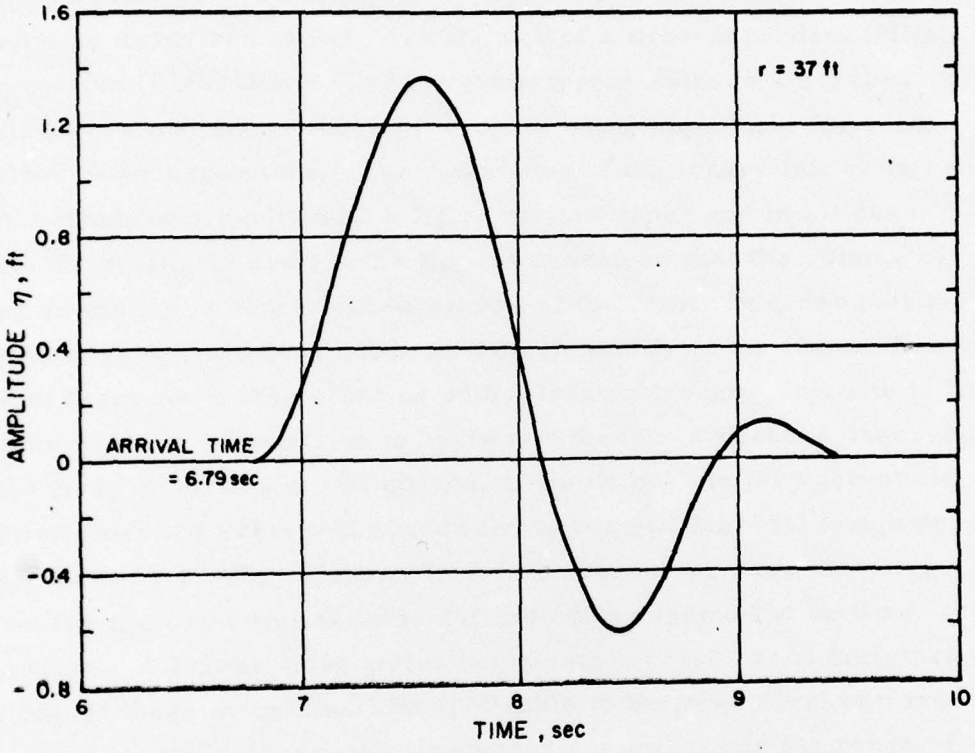

Figure 15
Time-dependent inital surface deformation,
truncated 4th degree curve for cavity and lip

PA-3-10217

applicability examined. Figures 2 and 4 illustrate the wave train from an assumed stationary cylindrical cavity and a truncated parabolic cavity. Obviously, and as expected, the models are inadequate for prediction purposes at large distances from the explosion because of the discontinuity at the front of the wave train. In addition, the calculations are inadequate near the explosion, requiring an improved numerical scheme as described in Ref. 4. The use of a time-dependent initial deformation (Figs. 3 and 5) of the same type results in a crest as the leading wave and shows more promise of being applicable for some shallow water explosions. The remainder of stationary initial deformations consist of a cavity with a lip of various types and in all cases (Figs. 6, 8, 10, 12 and 14) the lip was chosen so that the volume of water in the lip is equivalent to volume of the cavity in order that the resultant wave train does not have a discontinuity at the front. Naturally, each of these wave trains begins with a leading trough. In some of the regions where we would like to apply this theory, a crest is observed as the first disturbance. Of course, if we do not use the asymptotic solution (msp), a crest will appear first, but will start (although very small) at time $t = 0$. Figures 7, 9, 11, 13, and 15 show the wave trains for the same initial deformations when assumed to be time dependent. All these wave trains begin with a crest. It is anticipated that one of these models will be applicable to the prediction of waves generated by explosions in shallow water somewhere in the range of scaled depths of $0.6 \leq d/W^{1/3} \leq 6.0$. Unfortunately, no data are available for comparisons in the expected range of validity of these models.

NOMENCLATURE

a	wave height, first crest to trough
d	water depth
G	Green's Function
m	a wave number
P	pressure
R, R_1, R_2, R_3	crater radii
r	radial coordinate
T	wave period
t	time
W	explosive yield
x, y, z	spatial coordinates
η	wave amplitude
η_o	crater depth
τ	a dimensionless time
τ^*	a time parameter typical of the duration of water crater formation
φ	velocity potential

REFERENCES

1. Kajiura, K., "The Leading Wave of a Tsunami," Earthquake Research Bulletin of Japan

2. Whalin, R. W., "Contributions to the Mono Lake Experiments," NESCO Report S-256-2, Vol. II, October 1965

3. Whalin, R. W., "The Linear Theory of Water Waves Generated by Explosions," AGU Annual Meeting, April 1966, Washington, D. C.

4. Whalin, R. W., "Water Waves Produced by Underwater Explosions: Propagation Theory for Regions Near the Explosion," J. Geo. Res., Vol. 70, November 15, 1965, pp. 5541-5549